Validation of Unsteady Flamelet / Progress Variable Methodology for Non-premixed Turbulent Partially Premixed Flames

S. K. Sadasivuni[1], W. Malalasekera[1], S. S. Ibrahim[2]

[1]Wolfson School of Mechanical and Manufacturing Engineering, Loughborough University, Loughborough, LE113TU, Leicestershire, United Kingdom
[2]Deapartment of Automotive and Aerospace Engineering, Loughborough University, Loughborough, LE113TU, Leicestershire, United Kingdom

Abstract

This paper highlights the modeling capabilities of UFPV approach for the modeling of turbulent partially premixed lifted flames to capture the extinction and re-ignition phenomena. Large eddy simulation (LES) with the probability density function (PDF) approach provides the turbulence-chemistry interaction. All scalars are represented as a function of mean mixture fraction, mixture fraction variance, mean progress variable and scalar dissipation rate. Mixture fraction is assumed to follow a β-PDF distribution. Progress variable and scalar dissipation rate distributions are assumed to be a δ-PDF. Results are compared with experimental data of a vitiated co-flow burner with fuels like CH_4/Air and H_2/N_2. Results of radial plots for temperature, mixture fraction and scattered data of temperature with mixture fraction at various axial locations are compared. Lift-off height for a CH_4/Air flame appears to be over-predicted while the predicted lift-off height for a H_2/N_2 flame shows an under-prediction.

Introduction

Many combustion devices such as gas turbine engines and internal combustion engines are prone to operate in partially premixed mode of combustion. Flame lift-off and stabilization are found to be the two main issues in this mode of combustion. Standard combustion models based on fully premixed or fully non-premixed concepts are not exactly suitable for the modeling of partially premixed combustion situations. In this paper a suitably modified progress variable approach [1] is used to predict partially premixed lifted flames. The combustion model described in the present paper is tested using the LES approach for two experimental flame conditions to demonstrate its modeling capabilities in capturing important flame properties.

Laminar flamelet modeling introduced by Peters [2] and widely known as the steady laminar flamelet model (SLFM) is based on the fundamental concepts of Williams [3]. In this model a turbulent diffusion flame is assumed to be an ensemble of laminar stretched flamelets. This model has been validated in many studies [4-9]. One of the deficiencies of the SLFM as pointed out by Ferreira [9] is that SLFM model is not capable of predicting the flame extinction and re-ignition effects. SLFM has also been used for emission predictions with some success, Vranos *et al* [10]. Hossian and Malalasekera [11] have conducted SLFM based NO modeling for bluff body CH_4-H_2 flames and found to predict the NO mass fractions close to experimental values. Application of SLFM to LES has also been demonstrated and the methodology is now well established. These include Cook and Riley [12], Pierce and Moin [13], Branley and Jones [14], Kemp *et al* [15], Malalasekera *et al* [16]. However, the principle drawback of SLFM could be addressed only with the inclusion of unsteady effects in the flamelet calculations.

In situations where rapid changes in the scalar dissipation rate occur, use of the unsteady term in the flamelet equations is required in the calculations. The inclusion and importance of transient effects in flamelets models was identified by Haworth *et al* [17] and later Mauss *et al* [18] have demonstrated the use of unsteady flamelets to predict extinction and re-ignition in turbulent jet diffusion flames. Lagrangian flamelet model (LFM) was developed based on the transient flamelets and was extended further to account for the differential diffusion effects in the steady turbulent $CH_4/H_2/N_2$-air diffusion flame by Pitsch [19]. Importance of the transient effects has been emphasized by Pitsch and Steiner [20] with the application of unsteady flamelets to LES together with the LFM and the dynamic model of Pierce and Moin [13] for sub-grid variance of mixture fraction.

The partially premixed flamelet model of Peters [21] combines the flamelet models for non-premixed and premixed combustion. This model was extended to LES turbulent methane/air flames by Duchamp de Lageneste and Pitsch [22]. Flamelet progress variable (FPV) approach with typical SLFM combustion model has been tested by Pierce and Moin [1] where reaction progress variable was used instead of scalar dissipation rate to parameterize the flamelet library. Ihme *et al* [23] have studied the FPV model with a beta PDF for progress variable based on direct numerical simulation (DNS) data of turbulent non-premixed combustion. Recently, FPV model with steady flamelets has been applied using the RANS and LES framework for lifted flames with beta and delta PDFs for reaction progress variable by Ravikanti [24] and the results showed that the predicted flame lift off from the base and temperature predictions were very encouraging.

1* Corresponding author: mmsks@lboro.ac.uk

However an under-prediction of flame lift off height has been reported for the FPV model with LES calculations using the delta PDF of progress variable. All the above mentioned studies with FPV have been conducted considering the steady flamelet solution space.

Partially premixed flames are better predicted with the inclusion of unsteady effects in the flamelet solution. Therefore unsteady flamelet progress variable (UFPV) model, which combines the unsteady flamelet formulation with the progress variable approach, has been used to predict emissions like CO mass fraction by Pitsch and Ihme [25] with reasonable success. With this confidence, the present study considers the unsteady flamelet approach with the variations in scalar dissipation rate coupled with the progress variable approach. Here the model is used to predict the liftoff height and flame properties of partially premixed flames. With the beta PDF for progress variable the inclusion of scalar dissipation rate and beta PDF for mixture fraction in the lookup table considerably increases the computational space and time. In our work presented here, as a preliminary step towards developing the unsteady flamelet progress variable (UFPV) approach, a delta PDF for reaction progress variable is selected to keep the computational cost manageable and the UFPV model is applied to predict lifted flames. The objective of the present work is to validate the UFPV combustion model for partially premixed lifted flames and test the model with two different fuel compositions CH_4/Air and H_2/N_2 where experimental data is available.

Mathematical model outlining the governing equations of flow, turbulence and a detailed description of UFPV model of combustion, followed by the experimental details of the burner configuration are presented next. Following that the results of our LES are presented where the predictions for temperature and mixture fraction at different specified axial locations along the radial direction are compared with experimental data. Details of the flame liftoff and scattered data of temperature versus mixture fraction at selected planes of interest are also presented and discussed.

Mathematical Modeling

Turbulence and combustion modeling aspects are discussed in this section. Turbulent calculations based on LES and combustion modeling with UFPV is explained.

Turbulence Model

LES resolves the large scale turbulent motions which contain the majority of turbulent kinetic energy and control the dynamics of turbulence, whereas the small scales or sub-grid scales are modeled. The advantage of resolving the large scale motion is not applicable to chemical source term as the chemical time scales are smaller and therefore combustion needs to be modeled. However, LES seems to have the advantage due to its ability to predict accurately the intense scalar mixing process in any complex flow.

In LES, the governing equations of flow are resolved for the large scale features with the application of filters. The filtered field $\overline{f(x,t)}$ is determined by convolution with the filter function G.

$$\overline{f}(x) = \int_{\Omega} f(x')\, G(x-x', \overline{\Delta}(x))\, dx' \tag{1}$$

In the above expression, Ω represents the entire flow domain, $\overline{\Delta}$ is the filter width, which varies with the position. A top hat filter is used in the present study having a filter width $\overline{\Delta}_j$ set equal to the size Δx_j of the local cell. Favre filtering of all scalars is done in order to deal with the large fluctuations in density. Transport equations of mass, momentum and mixture fraction are Favre filtered and expressed as

$$\frac{\partial \overline{\rho}}{\partial t} + \frac{\partial \overline{\rho}\tilde{u}_i}{\partial x_j} = 0 \tag{2}$$

$$\frac{\partial \overline{\rho}\tilde{u}_i}{\partial t} + \frac{\partial (\overline{\rho}\tilde{u}_i \tilde{u}_j)}{\partial x_j} = -\frac{\partial \overline{P}}{\partial x_i} + \frac{\partial}{\partial x_j}\left[\overline{\rho}\nu\left(\frac{\partial \tilde{u}_i}{\partial x_j} + \frac{\partial \tilde{u}_j}{\partial x_i} \right) - \frac{2}{3}\overline{\rho}\frac{\partial \tilde{u}_k}{\partial x_k} \right] + \frac{\partial \tau_{ij}}{\partial x_j} \tag{3}$$

$$\frac{\partial \overline{\rho}\tilde{f}}{\partial t} + \frac{\partial}{\partial x_j}\left(\overline{\rho}\tilde{u}_j \tilde{f} \right) = \frac{\partial}{\partial x_j}\left[\overline{\rho}\left(\frac{\nu}{\sigma} + \frac{\sigma_t}{\sigma_t} \right)\frac{\partial \tilde{f}}{\partial x_j} \right] \tag{4}$$

In the above equations ρ is the density, u_i is the velocity component in x_i direction, p is the pressure, ν is the kinematic viscosity, f is the mixture fraction, ν_t is the turbulent viscosity, σ is the laminar Schmidt number and σ_t is the turbulent Schmidt number. An over-bar in the above equations describes the application of the spatial filter while the tilde denotes Favre filtered quantities. The laminar Schmidt number was set to 0.7 and the turbulent Schmidt number for mixture fraction was set to 0.4. Smagorinsky eddy viscosity model [26] is used to calculate the subgrid contribution to the momentum flux where the model constant C_s, strain rate tensor $S_{i,j}$ and filter width Δ are related as

$$\nu_t = C_s \Delta^2 \left| S_{i,j} \right| = C_s \Delta^2 \left| \frac{1}{2}\left(\frac{\partial \tilde{u}_i}{\partial x_j} + \frac{\partial \tilde{u}_j}{\partial x_i} \right) \right| \tag{5}$$

The value of model constant is calculated from the localised dynamic procedure of Piomelli and Liu [27].

A Brief Numerical Description

The present code was originally developed by Kirkpatrick [28] called as PUFFIN which was later modified by Ranga-Dinesh and Malalasekera [29] to incorporate the non-premixed jet flames using PDF approach. Transport equations are solved for spatially filtered continuity, momentum and a conserved scalar. The equations are discretised in space using the finite volume technique with a non-uniform Cartesian coordinated staggered grid arrangement. The spatial discretization involves a second order central differencing scheme for all the terms in the momentum and pressure correction equation. The diffusion terms are discretised with the second order central

differencing scheme for the mixture fraction transport equation, while the convection term is discretised using SHARP scheme of Leonard [30]. Crank-Nicolson scheme is used for appropriate approximation of the time derivative of the mixture fraction at the first instance. Variable density calculation based on an iterative time advancement scheme is used. The momentum equations are advanced using the new density field obtained at the end of each time step where the density is initially calculated from the PDF lookup table. A second order hybrid scheme is used for the integration of momentum equations with time. Advection terms are calculated using second order Adams-Bashforth scheme explicitly and diffusion terms are calculated using second order Adams-Moulton implicitly to obtain the velocity field. Pressure correction of VanKan [31] and Bell and Colella [32] is used for the mass conservation to obtain a divergence free velocity field. The time advancement is limited with the Courant number ranging from 0.3 to 0.6. The discretised linear algebraic equations are solved using the Bi-Conjugate Gradient Stabilized (BiCGStab) solver with Modified Strongly Implicit (MSI) preconditioner.

Unsteady Flamelet/Progress Variable Approach

UFPV approach is the extension of the flamelet progress variable (FPV) method. Preliminary studies of UFPV were performed by Pitsch and Ihme [25]. In FPV approach, steady flamelet equations are solved with scalar dissipation rate variations and are represented in the form of flamelets. But the scalar dissipation as a parameter is eliminated by the introduction of a new parameter called as flamelet progress variable (C). The flamelet model is based on the assumption that a turbulent diffusion flame is an ensemble of laminar flamelets where the introduction of conserved scalar, mixture fraction (*f*) is considered. The solution from the flamelet equations describes the dependency of all scalars like density, temperature and species mass fractions on the mixture fraction. The scalar dissipation rate is expressed as

$$\chi = 2D_Z \left(\nabla f\right)^2 \tag{6}$$

In the above expression, D_Z represents the molecular diffusivity of the mixture fraction. Solving the steady state flamelet equations, the state relation with any scalar ϕ can be given as

$$\phi = \phi\left(f, \chi_{st}\right) \tag{7}$$

The flamelet solution space can be represented with the S-shaped curve, which shows the stoichiometric temperature as the function of stoichiometric scalar dissipation rate. The three branches of the S-shaped curve are described as stable burning branch, unstable branch and non-burning or pure mixing branch as shown in Fig.1. From this figure it is clear that there exist multiple values or solutions for every single scalar dissipation rate. Therefore, a third parameter has to be defined which should parameterize the flamelet solution. Flamelet progress variable approach thus introduces a new flamelet parameter λ based on reactive scalar. The flamelet state solutions are parameterized with λ instead of scalar dissipation rate χ. This parameter identifies the unique state of each single flamelet along the S-shaped curve covering all the branches.

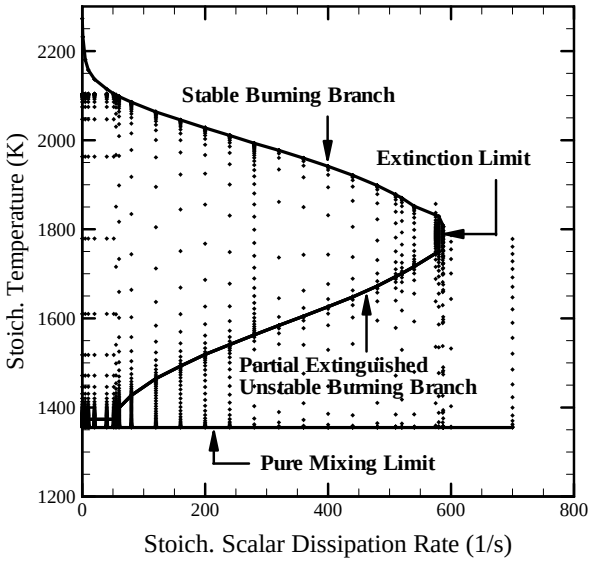

Fig.1 Unsteady flamelet solution space for CH_4/Air flame. Dotted values resemble the unsteady flamelet solutions at various scalar dissipation rates

Here the flamelet parameter λ is defined through the progress variable *C*, a reactive scalar introduced for the first time by Pierce and Moin [1]. In the present method the progress variable is taken as the summation of mass fraction of CO_2 and CO. The value of the flamelet parameter is defined as the maximum progress variable for each single flamelet solution. For every λ there exist a flamelet solution which is independent of mixture fraction and therefore the general scalar ϕ can be expressed as

$$\phi = \phi\left(f, \lambda\right) \tag{8}$$

Definition of λ provides the independent nature of f and λ which simplifies the joint PDF modeling of f and λ. The mean values of any scalar ϕ with the inclusion of Baye's theorem can be written as

$$\tilde{\phi} = \int_{\lambda_{\min}}^{\lambda_{\max}} \int_{0}^{1} \phi\left(f, \lambda\right) \tilde{P}\left(\lambda \mid f\right) \tilde{P}(f)\, df\, d\lambda \tag{9}$$

Where $\lambda_{\min}$ and $\lambda_{\max}$ are the limits corresponding to χ_{st} =0 and $\chi_{st} = \infty$. The joint PDF $\tilde{P}\left(f, \lambda\right)$ can be written as $\tilde{P}\left(f\right)\ \tilde{P}\left(\lambda\right)$. The PDF of mixture fraction $\tilde{P}\left(f\right)$ is assumed to follow beta distribution, Cook and Riley [12], Pierce and Moin [1] and Wall *et al.* [33]. Similarly, PDF of λ is approximated as delta in the present case, based on the studies conducted by Janicka and Kollmann [34]. Therefore, the mean scalar can now be represented as

$$\tilde{\phi} = \int_{\lambda_{\min}}^{\lambda_{\max}} \int_{0}^{1} \phi\left(f, \lambda\right) \tilde{P}\left(\lambda; \tilde{\lambda}\right) \tilde{P}(f; \tilde{f}, \widetilde{f''^2})\, df\, d\lambda \tag{10}$$

The transient solution of the flamelets is expected to predict the flame extinction and re-ignition phenomena in turbulent flows. The instantaneous drastic change in the scalar dissipation rate cannot be neglected for the turbulent flow which might not follow the instantaneous change in the temperature. In UFPV approach, flamelet parameter and scalar dissipation rate are independent parameters along with the mixture fraction for the construction of flamelet library. Therefore, each scalar dissipation rate has an individual distribution of flamelet parameter and mixture fraction. The flamelet library is constructed with all the extinguished and re-igniting flamelets. Fig. 1 shows the vertical dots that represent the unsteady flamelet solution, which are calculated with respect to time for different scalar dissipation rates from equilibrium to extinction. The flamelet library consists of all scalars which are dependent on mean mixture fraction, mixture fraction variance, progress variable and scalar dissipation rate. The flamelet library is produced from the flamelet generation methodology adopted by Pitsch and Fedotov [35] where the rate of change in temperature is positive on the left of S-shaped curve and negative on the right side. Here, in the present case we considered the flamelets till extinction. Therefore, we are focused on the left side of the S-shaped curve including the extinction limit. Flamelet calculations are performed using the steady state solutions on the unstable branch of the S-shaped curve as initial conditions. The value of the scalar dissipation rate is assumed to be slightly lower than that of steady state for the unsteady calculations. Because of the unstable nature of the middle branch, temperature increases to reach the stable branch. Similarly for the unsteady solution below the middle branch is obtained with a slight increase in the scalar dissipation rate as the initial solution. The vertical dots in Fig.1 represent the unsteady solution space which is later converted to a pre-integrated PDF table. The variable parameter here is time which is eliminated in UFPV approach, similar to elimination of scalar dissipation rate in FPV approach with the flamelet parameter λ . Thus the flamelet solution is now parameterized with mixture fraction *f,* flamelet parameter λ and stoichiometric scalar dissipation rate χ_{st} . The flamelet space for any scalar can be expressed as

$$\phi = \phi\left(f, \lambda, \chi_{st}\right) \tag{11}$$

The flamelet parameter and scalar dissipation rate are independent of mixture fraction and the three parameters are assumed to be independent of each other and thus the joint PDF can be expressed as

$$\tilde{P}\left(f, \lambda, \chi_{st}\right) = \tilde{P}\left(f\right)\tilde{P}\left(\lambda\right)\tilde{P}\left(\chi_{st}\right) \tag{12}$$

Similar to FPV approach, the distribution of mixture fraction is assumed to be beta PDF and a delta PDF distribution for flamelet parameter. The distribution of scalar dissipation rate is assumed to follow a delta PDF distribution. Hence the above equation can be represented as

$$\tilde{P}\left(f, \lambda, \chi_{st}\right) = \beta\left(f; \tilde{f}, \widetilde{f''^2}\right)\delta\left(\lambda - \lambda^*\right)\delta\left(\chi_{st} - \chi_{st}^*\right) \tag{13}$$

The complexity of solving λ^* and χ^* is eliminated by replacing the value of flamelet parameter λ by progress variable $\tilde{C}$ and stoichiometric scalar dissipation rate χ_{st} by mean scalar dissipation rate $\tilde{\chi}$, Pitsch and Ihme [25]. LES solves the equations of conserved scalar and progress variable to obtain the mean values of mixture fraction $\tilde{f}$, its variance $\widetilde{f''^2}$, progress variable $\tilde{C}$ and scalar dissipation rate $\tilde{\chi}$. Flamelet parameter is normalized to vary from 0 to 1. The re-mapping technique of Ravikanti [24] is used here for conversion of flamelet parameter to progress variable. The mean progress variable obtained from the LES is made equal to the progress variable calculated from the pre-integration PDF table as the only constraint. We thus obtain the filtered scalars as a function of $\tilde{f}, \widetilde{f''^2}, \tilde{C}$ and $\tilde{\chi}$. These four parameters are obtained as the mean values from LES which are interpolated for obtaining the mean scalars from the PDF lookup table.

The unsteady flamelet solutions are obtained from FlameMaster code developed by Pitsch [36]. The chemistry involved in the code includes GRI 2.11 mechanism for methane based fuels with the assumption of unity Lewis numbers for all the species without the radiation effect. Hydrogen mechanism involved in the H_2/N_2 case is based on the reduced kinetic mechanism developed by Peters and Rogg [37].

Experimental Details

The validation of the combustion model is done with the comparison of experimental data available from the lifted flame of Cabra *et al* [38]. The burner has two set of experimental data for different fuel compositions. The first set of data is for CH_4/Air as the fuel jet inlet with vitiated co-flow of H_2/Air and second set is for H_2/N_2 as fuel and H_2/Air as co-flow inlet. The present combustion model is applied for both these configurations and results are compared with experiments. The burner consists of a central nozzle with inner diameter (*D*) of 4.57 mm and outer diameter of 6.35 mm. A perforated plate of 210 mm diameter through which vitiated co-flow of air is issued surrounds the central nozzle. A flow blockage of 85% was reported with 2200 holes drilled in it. The vitiated co-flow consists of products of lean premixed H_2/Air flame with an equivalence ratio of 0.4. The entrainment of ambient air into the co-flow has been delayed by incorporating an exit collar which surrounds the perforated plate. The fuel jet consisting of a mixture of 33% CH_4 and 67% air is issued from the central nozzle for the first set of data and 25% H_2 and 75% N_2 for the second. The details of the burner can be depicted from Fig.2. Table 1 shows the details of the two fuel compositions and their inlet conditions.

Computational Details

The computational domain has dimensions of 200 x 200 x 410 (all dimensions are in mm). The axial distance of approximately 90 jet diameters and the

burner width of approximately 44 jet diameters is used in order to account the independency of flow entrainment from the surroundings.

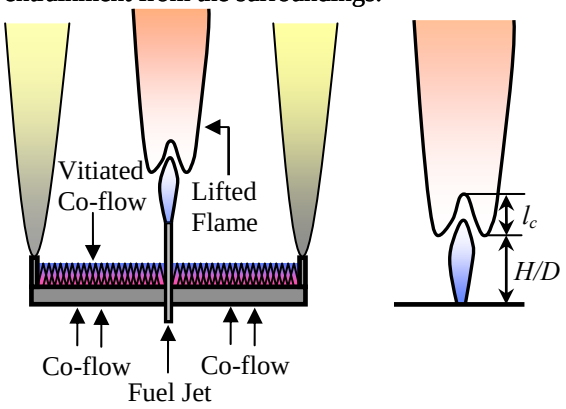

Fig.2 Schematic of burner configuration

An inlet jet velocity is specified with a $1/7^{th}$ power law profile. Convective outlet boundary condition is used at the outlet surface and all the walls and co-flow boundaries in the domain have been treated as adiabatic. Cartesian staggered non-uniform grid distribution of 85 x 85 x 150 in the X, Y and Z directions to discretize the domain is used. The grid details are depicted in the Fig.3.

Table.1 Details of the two flame configurations

	H_2/N_2 Flame		CH_4/Air Flame	
	Jet	Co-flow	Jet	Co-flow
Re	23,600	18,600	28,000	23,300
V (m/s)	107	3.5	100	5.4
T (K)	305	1045	300	1355
X_{O2}	0.0021	0.15	0.15	0.12
X_{N2}	0.74	0.75	0.52	0.73
X_{H2O}	0.0015	0.099	0.0029	0.15
X_{OH}(ppm)	<1	<1	<1	200
X_{H2}	0.25	5 x 10^{-4}	100	100
X_{CH4}	-	-	0.33	0.0003
f_{st}	0.47		0.17	

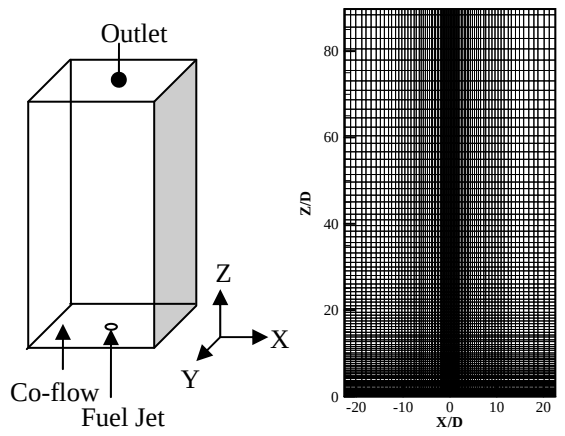

Fig.3 Details of computational domain and grid

An ignition source is provided with the progress variable of 0.9 patched in the region of best mixed fuel air mixture. A total time of 60 ms is allowed to run the unsteady simulation, out of which first 40 ms is utilized to develop the flow to establish. Remaining 20ms is used for collection of statistics and the averaged data for this time is used for post-processing of results.

Results and Discussion

This section is divided in two set of results. Initially, the predictions for the CH_4/Air flame are discussed and later with H_2/N_2 flame. Both include the radial comparisons for temperature and mixture fraction at different axial locations along the burner. Scattered data is also compared at the locations of interest for the prediction of flame extinction and re-ignition. The flame lift off is compared for both the flames with their corresponding experimental values.

CH_4/Air Flame

The radial mean mixture fraction and temperature plots at z/D locations of 1.0, 15.0, 30.0, 40.0, 50.0 and 70.0 are depicted in Fig.4 and Fig.5 respectively. The locations z/D = 40.0, 50.0 and 70.0 on the downstream of the burner are the positions where predictions are difficult to capture numerically as the flame is more dynamic and unstable.

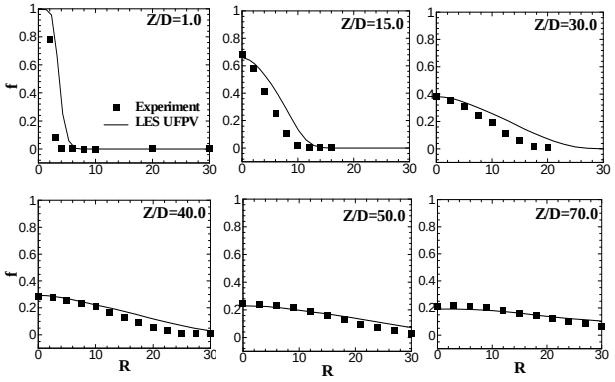

Fig.4 Radial plot comparison of mean mixture fraction at different axial locations for CH_4/Air flame

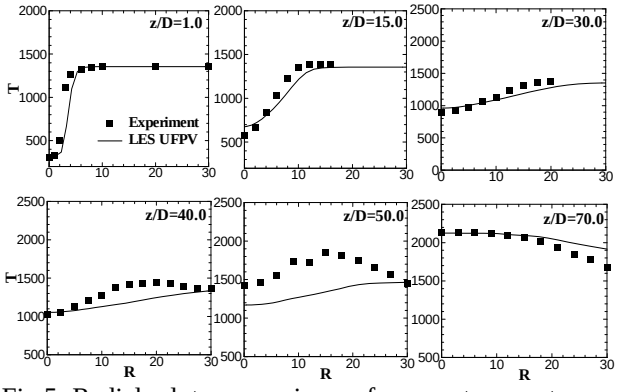

Fig.5 Radial plot comparison of mean temperature at different axial locations for CH_4/Air flame

Mixture fraction is slightly over-predicted at the first three locations but the predictions at remaining locations are well captured. Temperature predictions are resonably good at the first three locations, but under-predicted at locations z/D={40.0,50.0}. As mentioned earlier in this zone the flame is highly

fluctuating and subjected to extintion and re-ignition. At the last location z/D=70.0, centreline temperature is found to be very close to the experiments. Overall, it can be seen that except at the location z/D=50.0 predictions are reasonably good. The model appears to be partially successful in capturing extinction and re-ignition effects.

The flame lift-off (Fig.6) in the present paper is considered as the height from the base where the temperature is equal to the co-flow temperature (1355K). Lift-off height is represented in terms of H/D where H is the axial distance from the base of the burner jet. Experimentally found value of H/D is 35 which was captured visually based on the flame luminosity. Numerical lift-off is found to be around 42. The discrepancy of the lift off height with experiments is about 20 %. This over-prediction may be due to the highly fluctuating nature of the flame and the temperature that has been chosen to obtain this height. A better lift-off height can be represented with OH mass fraction contours, but the present simulation is limited to calculation of mixture fraction and temperature and minor species have not been considered in the look-up table.

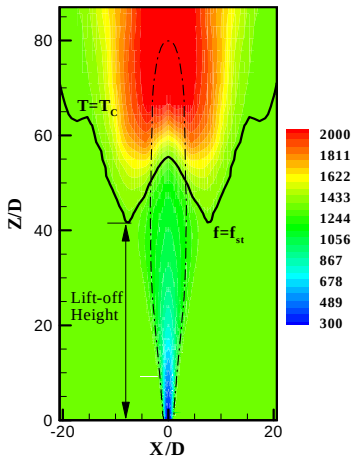

Fig.6 Mean temperature contour plot showing the flame lift-off for CH_4/Air flame

Flame extinction and re-ignition can be represented by plotting scattered data of temperature versus mixture fraction. Data is collected for all the axial location planes of interest and found that locations z/D={50.0,70.0} are prone to maximum flame instability where flame fluctuates with near blow-off and re-attaching features. Fig.7 shows scattered data for temepearture at the last locations z/D=50.0 and 70.0. Left hand side figures represent experimental data and the right hand side plots shows the numerical calculations. At location z/d=70 conditions are almost close to equilibrium and compare reasonably well with experiments with marginal under-prediction in peak temperatures close to equilibrium. Experimentally observed lift-off is 35. Experimentally the temperatures vary from equilibrium to mixing as the flame tries to detach and re-ignite in the regions from H/D~35 to 60. The numerical simulation shows a lift-off of around 42. This suggests that numerical comparison at the location z/D=50.0 is most likely to show data biased towards mixing hence the observed discrepancy.

Scattered data is compared only at locations z/D={50.0,70.0}. Any location below z/D=50.0 should resemble only pure mixing limit. At the location plane z/D=50.0, the maximum temperature close to equilibrium is under-predicted but the mixture fraction predictions agree well at all locations. Reasonably good agreement with the experiments for temperature at most locations except at z/D=50.0 shows the capability of the UFPV approach for the modeling of lifted flame physics.

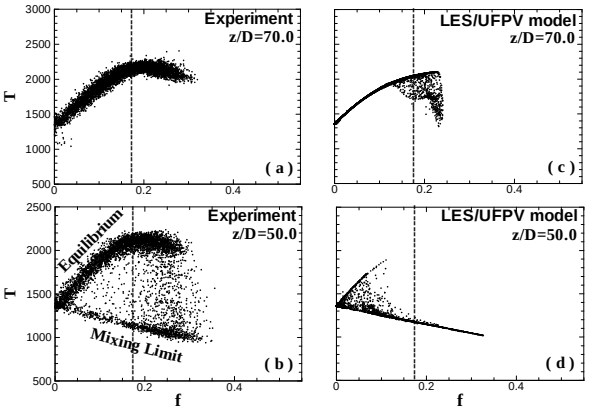

Fig.7 Scattered temperature plotted against mixture fraction at different axial locations

H_2/N_2 Flame

The structure of the H_2/N_2 lifted turbulent flame is investigated by examing the comparisons at the axial locations z/D={1.0,8.0,9.0,10.0,11.0,14.0}. The mean mixture fraction at these locations is found to be very well predicted as shown in Fig.8. It is however clear that there is a very marginal over-prediction radially but the overall comparison with the experimental data is very encouraging. Mixture fraction and temperature are closely related to the unsteady flamelet solution. Therefore, any marginal discrepancy in the mixture fraction predictions should alter the mean radial temperatures. Fig.9 shows the radial plot comparisons for temperatures at different axial locations. Eventhough the mixture fraction predictions are good, temperature plots show an over-prediction at locations z/D={1.0 to 10.0} radially at around 6~9mm. Calculated temperature rise and drop at this radial distance indicates that the flame base is not lifted but attached to jet exit. At the same radial location experimental data shows that there is no drastic change in the temperature because the observed lift-off found experimentally is H/D=10. At location z/D=11.0 the peak rise in temperature is numerically predicted well. Fig.10 depicts the flame attachment almost close to the base with a minimal flame lift based on the co-flow temperature boundary line (1045K). Numerically calculated lift off would be in the order of x/D=1. This is considerable under-prediction. The temperature range from minimum to maximum is 1045 to 1500 K (a very narrow range), therefore from a temperature contour

alone it is difficult to judge accaurate lift off height.

Based on overall observations, the present combustion model can be used for the simulation of lifted flames. Futher improvements to this model can be made (i) by the inclusion of radiation, (ii) calculation of the lift off height based on OH contours, (iii) changing the definition of progress variable.

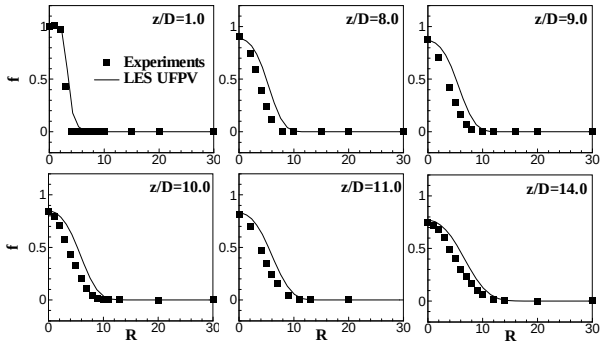

Fig.8 Radial plot comparison of mean mixture fraction at different axial locations for H_2/N_2 flame

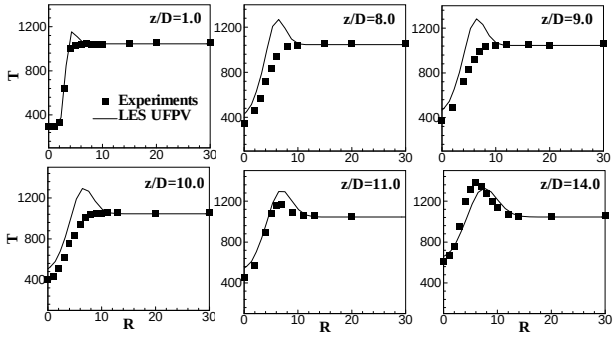

Fig.9 Radial plot comparison of mean temperature at different axial locations for H_2/N_2 flame

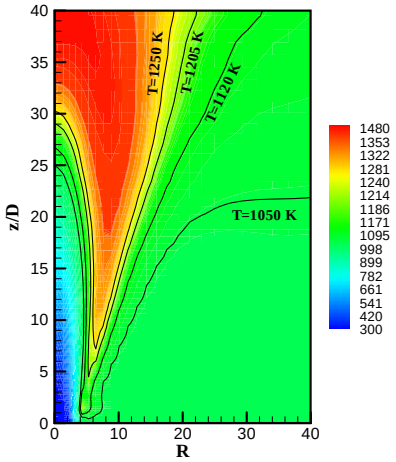

Fig.10 Mean temperature contours at the centre plane (x=0) for H_2/N_2 flame

Conclusions

In this work a combustion model based UFPV approach has been applied for the modeling of a lifted flame burner. Two different flame conditions were used to test the model capabilities. Overall the model appears predict reasonably good mixture fraction and temperature distribution at all locations of the flame. Predicted lift-off height is also reasonably close to experimental observations. Success in the temperature and mixture fraction predictions is encouraging. UFPV model is found to predict better predictions for methane based flames rather than hydrogen based. An over-prediction of lift-off for the methane based flame and an under-prediction in lift-off height for hydrogen flame was observed. But radial plot comparison showed reasonably good predictions for temperature and mixture fraction for both the flames. Hence, UFPV can be applied with confidence for partially premixed lifted flames.

Acknowledgements

The author is very thankful to Dr. Murthy Ravikanti for providing the baseline code for PDF file generation. Also very grateful for the support provided by Dr. H. Pitsch, Stanford University, US, with his FlameMaster code for the generation of unsteady flamelets.

References

[1] C.D. Pierce, P. Moin, Journal of Fluid Mechanics 504 (2004) 73-97.
[2] N. Peters, Progress in Energy and Combustion Science, 10 (1984) 319-339.
[3] F.A. Williams, Turbulent Mixing in Non-reactive and Reactive Flows, New York, Plenum Press (1975) 189-208.
[4] N. Peters, Combustion Science and Technology 30 (1983) 1-17.
[5] P.T. Roberts, J.B. Moss, Eighteenth Symposium (International) on Combustion/The Combustion Institute 941 (1981).
[6] C. Drake, Twenty-first Symposium (International) on Combustion/The Combustion Institute (1986) 1579-1589.
[7] S.K. Liew, K.N.C. Bray, J.B. Moss, Combust. Flame 56 (1984) 199-213.
[8] M. Hossain, CFD Modeling of Turbulent Non-premixed Combustion, Ph.D Thesis, Loughborough University, UK., 1999.
[9] J.C. Ferreira, Progress in Computational Fluid Dynamics 1 (2001) 29-42.
[10] A. Vranos, B.A. Knight, W.M. Proscia, L. Chiappetta, M.D. Smooke, Twenty Fourth Symposium (International) on Combustion/The Combustion Institute (1992) 377-384.
[11] M. Hossain, W. Malalasekera, Journal of Power and Energy 217 (2003) 201-210.
[12] A.W. Cook, J.J. Riley, Physics of Fluids 6 (1994) 2868-2870.
[13] C.D. Pierce, P. Moin, Physics of Fluids 10 (1998) 3041-3044.
[14] N. Branley, W.P. Jones, Engineering Turbulence Modeling and Experiments, In W. Rodi and D. Laurence (Eds.), Amsterdam: Elsevier Science 4 (1999) 861-870.
[15] A. Kempf, W. Malalasekera, K.K.J. Ranga-Dinesh, O. Stein, Flow Turbulence and Combustion 81 (2008) 523-561.
[16] W. Malalasekera, K.K.J. Ranga-Dinesh, S.S. Ibrahim, A.R. Masri, Combustion Science and Technology 180(5) (2008) 809-832.
[17] D.C. Haworth, M.C. Drake, S.B. Pope, R.J. Blint, Twenty Second Symposium (International) on Combustion/The Combustion Institute (1988) 589-597.
[18] F. Mauss, D. Keller, N. Peters, Twenty Third Symposium (International) on Combustion/The Combustion Institute (1990) 693- 698.

[19] H. Pitsch, M. Chen, N. Peters, Twenty Seventh Symposium (International) on Combustion/The Combustion Institute (1998) 1057- 1064.
[20] H. Pitsch, H. Steiner, Physics of Fluids 12 (2000) 2541-2554.
[21] N. Peters, Journal of Fluid Mechanics 384 (1999) 107-132.
[22] L. Duchamp de Lageneste, H. Pitsch, Annual Research Briefs, Centre for Turbulence Research, NASA Ames/Stanford University (2001) 97-107.
[23] M. Ihme, C.M. Cha, H. Pitsch, Thirtieth Symposium (International) on Combustion/The Combustion Institute (2005) 793-800.
[24] H. Pitsch, M. Ihme, AIAA Paper (2005) 2004-557.
[25] V.V.S.M. Ravikanti, Advanced Flamelet Modeling of Turbulent Non-premixed and Partially Premixed Combustion, Ph.D Thesis, Loughborough University, UK., 2008.
[26] J. Smagorinsky, General Circulation Experiments with the Primitive Equations, Part-I: The Basic Experiment, Monthly Weather Review 91 (1963) 99-164.
[27] U. Piomelli, J. Liu, Physics of Fluids 7 (1995) 839-848.
[28] M.P. Kirkpatrick, A Large Eddy Simulation Code for Industrial and Environmental Flows, Ph.D Thesis, University of Sydney, Australia., 2002.
[29] K.K.J. Ranga Dinesh, W. Malalasekera, S.S. Ibrahim, M.P. Kirkpatrick, Proceedings of the 5th International Symposium on Turbulence, Heat and Mass Transfer (2006) 1-7.
[30] B.P. Leonard, Sharp Simulation of Discontinuities in Highly Convective Steady Flow, NASA Technical Report (1987) 100240.
[31] J. VanKan, SIAM Journal of Scientific and Statistical Computing 7 (1986) 870-891.
[32] J.B. Bell, P. Colella, Journal of Computational Physics 85 (1989) 257-283.
[33] C. Wall, B. Boersma, P. Moin, Physics of Fluids 12(10) (2000) 2522-2529.
[34] J. Janicka, W. Kollmann, Proceedings of Combustion Institute 17 (1978) 421-430.
[35] H. Pitsch, S. Fedotov, Combustion Theory and Modeling 5 (2001) 41-57.
[36] H. Pitsch, A C++ Computer Program for 0-D and 1-D Laminar Flame Calculations, RWTH Aachen (1998).
[37] N. Peters, B. Rogg, Lecture Notes in Physics-Reduced Kinetic Mechanisms for Applications in Combustion Systems, Springer, 1993.
[38] R. Cabra, J.-Y. Chen, R.W. Dibble, A.N. Karpetis, R.S. Barlow, Combust. Flame 143 (2005) 491-506.